RESEARCH ARTICLE | *Vascular Biology and Microcirculation*

Important role of endothelium-dependent hyperpolarization in the pulmonary microcirculation in male mice: implications for hypoxia-induced pulmonary hypertension

Shuhei Tanaka, Takashi Shiroto, Shigeo Godo, Hiroki Saito, Yosuke Ikumi, Akiyo Ito, Shoko Kajitani, Saori Sato, and Hiroaki Shimokawa

Department of Cardiovascular Medicine, Tohoku University Graduate School of Medicine, Sendai, Japan

Submitted 2 August 2017; accepted in final form 29 December 2017

Tanaka S, Shiroto T, Godo S, Saito H, Ikumi Y, Ito A, Kajitani S, Sato S, Shimokawa H. Important role of endothelium-dependent hyperpolarization in the pulmonary microcirculation in male mice: implications for hypoxia-induced pulmonary hypertension. *Am J Physiol Heart Circ Physiol* 314: H940–H953, 2018. First published January 5, 2018; doi:10.1152/ajpheart.00487.2017.—Endothelium-dependent hyperpolarization (EDH) plays important roles in the systemic circulation, whereas its role in the pulmonary circulation remains largely unknown. Furthermore, the underlying mechanisms of pulmonary hypertension (PH) also remain to be elucidated. We thus aimed to elucidate the role of EDH in pulmonary circulation in general and in PH in particular. In isolated perfused lung and using male wild-type mice, endothelium-dependent relaxation to bradykinin (BK) was significantly reduced in the presence of N^{ω}-nitro-L-arginine by ~50% compared with those in the presence of indomethacin, and the combination of apamin plus charybdotoxin abolished the residual relaxation, showing the comparable contributions of nitric oxide (NO) and EDH in the pulmonary microcirculation under physiological conditions. Catalase markedly inhibited EDH-mediated relaxation, indicating the predominant contribution of endothelium-derived H_2O_2. BK-mediated relaxation was significantly reduced at *day 1* of hypoxia, whereas it thereafter remained unchanged until *day 28*. EDH-mediated relaxation was diminished at *day 2* of hypoxia, indicating a transition from EDH to NO in BK-mediated relaxation before the development of hypoxia-induced PH. Mechanistically, chronic hypoxia enhanced endothelial NO synthase expression and activity associated with downregulation of caveolin-1. Nitrotyrosine levels were significantly higher in vascular smooth muscle of pulmonary microvessels under chronic hypoxia than under normoxia. A similar transition of the mediators in BK-mediated relaxation was also noted in the Sugen hypoxia mouse model. These results indicate that EDH plays important roles in the pulmonary microcirculation in addition to NO under normoxic conditions and that impaired EDH-mediated relaxation and subsequent nitrosative stress may be potential triggers of the onset of PH.

NEW & NOTEWORTHY This study provides novel evidence that both endothelium-dependent hyperpolarization and nitric oxide play important roles in endothelium-dependent relaxation in the pulmonary microcirculation under physiological conditions in mice and that hypoxia first impairs endothelium-dependent hyperpolarization-mediated relaxation, with compensatory upregulation of nitric oxide, before the development of hypoxia-induced pulmonary hypertension.

endothelium-dependent hyperpolarization; hypoxia; pulmonary microcirculation

INTRODUCTION

Pulmonary arterial hypertension (PAH) is a progressive vasculopathy characterized by specific histological changes, including intimal and medial wall thickness, muscularization of distal pulmonary arteries, and concentric obliterative and plexiform lesions (38). These structural changes increase pulmonary arterial resistance and pressure, resulting in the development of right ventricular (RV) failure and premature death (31, 32). However, the trigger(s) of these vascular disorders still remains unclear. Endothelial dysfunction, including decreased bioavailability of PGI_2 and nitric oxide (NO) and also increased activity of endothelin and thromboxane, has been considered a key underlying mechanism of pulmonary vascular remodeling in PAH (9, 15, 26, 34, 67). Indeed, a variety of vasodilatory therapies targeting these mediators attributable to endothelial dysfunction have been developed, including PGI_2 and its analogs (3, 61), inhalation of NO (30, 39), soluble guanylyl cyclase (sGC) modulators (23, 24), selective phosphodiesterase 5 (PDE5) inhibitors (20), and endothelin receptor antagonists (56). They are beneficial for some patients with PAH by reducing pulmonary arterial pressure and improving long-term survival (38). However, many patients with PAH still die or need lung transplantation even with these therapies (31). Thus, a new therapeutic target remains to be elucidated to improve long-term survival of PAH patients.

The endothelium regulates vascular tonus by synthesizing and releasing endothelium-derived relaxing factors (EDRFs), including vasodilator PGs (mainly PGI_2), NO, and endothelium-dependent hyperpolarization (EDH) factor (59). We (39) have previously demonstrated that the contribution of EDRFs varies depending on blood vessel size; NO plays an important role in relatively large arteries, whereas the importance of EDH increases as vessel size decreases. In contrast, PGI_2 has a minor but constant role regardless of vessel size (60). Thus, it is conceivable that EDH is involved in the regulatory mechanisms of arterial blood pressure and organ perfusion in systemic circulation (59). We also have previously demonstrated that endothelium-derived H_2O_2 is an important EDH factor in several arteries in animals and humans (43–45). Although NO and EDH are well balanced in a distinct vessel size-dependent manner under phys-

Address for reprint requests and other correspondence: H. Shimokawa, Dept. of Cardiovascular Medicine, Tohoku Univ. Graduate School of Medicine, 1-1 Seiryo-machi, Aoba-ku, Sendai 980-8574, Japan (e-mail: shimo@cardio.med.tohoku.ac.jp).

iological conditions, the physiological balance between NO and EDH can be disrupted under various pathological conditions, such as aging, dyslipidemia, and hypertension, leading to enhanced vasoconstriction and the initial step toward cardiovascular diseases (69). For example, in a chronic cardiac pressure overload model, the disruption of the physiological balance between NO and EDH exhibited reduced survival rate, impaired coronary flow reserve, and enhanced myocardial hypoxia in mice in vivo (28). Thus, not only NO but also EDH plays important roles in regulating vascular tonus and maintaining cardiovascular homeostasis in systemic circulation. However, the role of EDH in the pulmonary microcirculation remains to be clarified.

In the present study, we thus aimed to examine the role of EDH in the pulmonary microcirculation in general and in pulmonary hypertension (PH) in particular. We tested our hypothesis that EDH plays a primary role in the pulmonary microcirculation under physiological conditions and that its role is altered during the development of hypoxia-induced PH in mice in vivo. Although it is generally known that female sex is a risk factor for PAH (66), we used only male mice in the present study along with our previous reports on systemic circulation to examine the differences between the pulmonary and systemic circulations.

METHODS

Animals. Experiments were conducted in 11- to 16-wk-old male C57BL/6 mice (~25 g body wt under normoxia). This study was reviewed and approved by the Committee on Ethics of Animal Experiments of Tohoku University (2015MdA-281) based on *Animal Research*: Reporting of In Vivo *Experiments* guidelines. Male C57BL/6 mice were purchased from CLEA Japan (Tokyo, Japan). All animals were cared for in accordance with the rules and regulations configured by the committee, fed normal chow, and maintained on a 12:12-h light-dark cycle.

Wire myograph. We measured isometric tensions of the first to second branches of the intrapulmonary arteries (~300–500 μm in external diameter) as previously described (14). After mice had been anesthetized with intraperitoneal injection of pentobarbital sodium (50 mg/kg), the intrapulmonary arteries were carefully isolated under a microscope, cut into 1-mm-long rings without adventitia, and mounted in a wire myograph (620M, Danish Myo Technology, Aarhus, Denmark). Each arterial ring was bathed in organ chambers filled with 5 ml of Krebs-Henseleit buffer (KHB) warmed to 37°C and aerated with 95% O_2 and 5% CO_2 and then stretched to optimal resting tension, which was determined in preliminary experiments (data not shown). After a 60-min equilibration period, rings were challenged with KCl (60 mmol/l) to test for their viability; rings that were able to generate over 1 mN of force were allowed for the following isometric tension recordings. In a preliminary study, we obtained cumulative dose-response curves to U46619, a thromboxane A_2 mimetic ($10^{-8}-10^{-4.5}$ mol/l), and obtained the concentration of U46619 to cause 50% contraction (EC_{50}: -7.35 ± 0.08 log mol/l). After a washout and a 30-min recovery period, rings were precontracted with the EC_{50} concentration of U46619 to examine the relaxation in response to cumulative addition of acetylcholine (ACh; $10^{-10}-10^{-5}$ mol/l). Relaxation to ACh was calculated as percentages of the precontracted levels induced by U46619. The contributions of PGI_2, NO, and EDH to ACh-induced relaxation were determined by the inhibitory effect of indomethacin (Indo; cyclooxygenase inhibitor, 10^{-5} mol/l), N^{ω}-nitro-L-arginine [L-NNA; NO synthase (NOS) inhibitor, 10^{-4} mol/l], and a combination of apamin [Apa; small-conductance Ca^{2+}-activated K^+ (SK_{Ca}) channel blocker, 10^{-6} mol/l] and charybdotoxin [CTx; intermediate-conductance (IK_{Ca}) and large-conductance Ca^{2+}-activated K^+ (BK_{Ca}) channel blocker, 10^{-7} mol/l], respectively (28). All inhibitors were applied to the organ chambers 30 min before precontraction with U46619. Responses were continuously monitored (PowerLab 8/30 computer system, AD Instruments, Colorado Springs, CO) and were analyzed by a computer-based analysis system in LabChart 7.0 software.

Isolated perfused lung model. For perfusion and ventilation, an open-chest mouse lung preparation was used as previously described in detail (62, 75). Mice were pretreated intraperitoneally with heparin (100 U) and then, after 10 min, anesthetized by intraperitoneal injection of pentobarbital sodium (50 mg/kg). They were then intubated and positively ventilated with a gas mixture containing 95% O_2 and 5% CO_2 at 6 ml/kg tidal volume at a rate of 120 breaths/min (MiniVent Mouse Ventilator 845, Harvard Apparatus, Holliston, MA). A sternotomy was performed, cannulas were inserted into the main pulmonary artery and left ventricle, and the main pulmonary artery, aorta, and ventricles were ligated simultaneously, making the lungs completely isolated from the hearts. After cannulation, the lungs were perfused with warmed KHB containing 5% BSA through the pulmonary arterial cannula at a constant flow (0.08 ml$\cdot$min$^{-1}\cdot$g body wt^{-1}) using a peristaltic pump (Minipuls 3, Gilson Medical Electronics, Middleton, WI). The lungs were flushed for 9 min to remove blood and to gradually increase the target flow rate before establishing recirculation. Left atrial pressure was maintained at ~4 mmHg by adjusting the distance between the lung and the outlet of the cannula inserted in the left ventricle. Pulmonary arterial pressure was monitored and recorded using a pressure transducer connected to a side port of the pulmonary arterial cannula (PowerLab 8/30 computer system). We assumed the pulmonary venous pressure to be zero (1). To clarify the responses to each agonist, each lung preparation was used to study with only one dose of each agonist. After the 30-min equilibration period, the lungs were precontracted with U46619, and then vascular responses were examined. U46619 cumulative dose-response curves ($10^{-8}-10^{-4.5}$ mol/l) were performed, and the concentration of U46619 required to produce a 50% response (EC_{50}) was used to precontract the vessels for subsequent vasorelaxation. We adjusted the degree of precontraction in each preparation to precontracted levels of the normoxic lungs in the absence of any inhibitors. To assess endothelium-dependent relaxation, bradykinin (BK; 10^{-5} mol/l) was used. The dose of BK was predetermined by experiments that BK elicited the maximal relaxation in the control lungs (data not shown). To assess endothelium-independent relaxation, sodium nitroprusside (SNP; 10^{-5} mol/l), a NO donor, was used. Vascular responses to exogenous H_2O_2 (10^{-4} mol/l) were examined in the presence of Indo (10^{-5} mol/l) and L-NNA (10^{-4} mol/l). Relaxations to vasodilators were calculated as percentages of the increased pressure induced by U46619. The inhibitory effects of Indo, L-NNA, the combination of Apa and CTx, and catalase (12,500 U/ml) were examined. All inhibitors were administered from the start of perfusion. We calculated basal vascular resistance as the value given by baseline perfusion pressure (in mmHg)/flow (in ml/min). Each surgical preparation before perfusion needed ~6 min, and each procedure took ~2 h. A few lungs exhibited massive edema and were excluded.

Hypoxia-induced PH model. A hypoxic exposure model was used to assess the effect of hypoxia on the relaxation of pulmonary arteries in mice (57). Briefly, 10- to 12-wk-old male wild-type (WT) mice on a normal chow diet and under a 12:12-h light-dark cycle were exposed to hypoxia (10% O_2) for 1, 2, 7, 14, or 28 days. Hypoxic mice were housed in an acrylic chamber with a nonrecirculating gas mixture of 10% O_2 and 90% N_2 by adsorption-type oxygen concentrator to use exhaust air (Teijin, Tokyo, Japan), whereas normoxic mice were housed in room air (21% O_2). All hypoxic mice were studied within 1 h of removal from the chamber.

Western blot analysis. We performed Western blot analysis as previously described (48). After perfusion with cold KHB, the lungs were isolated and snap frozen. Frozen lungs were then lysed in tissue protein extraction reagent (T-PER, ThermoFisher, Rockford, IL) con-

taining protease inhibitor cocktail (Sigma-Aldrich, St. Louis, MO) followed by homogenation and centrifugation. The supernatants from lung homogenates were loaded with SDS-PAGE and transferred to PVDF membranes (GE Healthcare, Fairfield County, CT) after being blocked for 1 h at room temperature. The primary antibodies used were as follows: α-tubulin (1:10,000, Sigma-Aldrich), endothelial NOS [eNOS (1:5,000, BD transduction Laboratories, San Jose, CA)], phosphorylated (p)Ser^{1177}-eNOS (1:400, BD transduction Laboratories), pThr^{495}-eNOS (1:400, BD transduction Laboratories), pSer^{239}-vasodilator-stimulated phosphoprotein [VASP (1:500); Abcam, Cambridge, UK], total VASP (1:1,000, Abcam), and caveolin-1 [Cav-1 (1:1,000), Cell Signaling Technology, Danvers, MA]. The regions containing proteins were visualized by the enhanced chemiluminescence system (ECL Prime Western Blotting Detection Reagent, GE Healthcare). Densitometric analysis was performed with ImageJ software (National Institutes of Health, Bethesda, MD).

Immunoprecipitation. After perfusion with cold KHB, the lungs were isolated and snap frozen. Frozen lungs were lysed in T-PER (ThermoFisher) containing protease inhibitor cocktail (Sigma-Aldrich) followed by homogenation and centrifugation. The supernatants were incubated with anti-eNOS antibody at a dilution of 1:100 for 1 h at 4°C. After the incubation, 25 μl of prewashed EZ View Protein G Affinity gel (Sigma-Aldrich) were added to the lysates followed by incubation for 1 h at 4°C. After centrifugation, the supernatants were removed. After being washed three times with lysis buffer, 50 μl of sample buffer (10% SDS, 30% 2-melcaptoethanol, 20% glycelol, and 0.1% bromophenol blue) were added and heated to 95°C for 5 min followed by centrifugation. The supernatants were analyzed by immunoblot analysis (50).

Right heart catheterization. After 1, 2, 7, 14, or 28 days of exposure to hypoxia (10% O_2) or normoxia, mice were anesthetized with isoflurane (1.0%). To examine the development of PH, we measured RV systolic pressure (RVSP) and RV end-diastolic pressure (RVEDP). For right heart catheterization, a 1.2-Fr pressure catheter (Scisense, London, ON, Canada) was inserted into the RV through the right jugular vein to measure RVSP and RVEDP. All data were analyzed using the PowerLab 8/30 computer system and averaged over 10 sequential beats (57).

Histological analysis. After right heart catheterization, the lungs were rigorously and completely perfused with cold KHB at physiological pressure until the color of the lungs clearly showed white. They were then fixed in 10% formaldehyde solution for 24 h on a shaker at room temperature. After serial steps of washing and dehydration, the whole lungs were embedded in paraffin, and cross sections (3 μm) were prepared. Paraffin sections were stained with elastica-Masson. Pulmonary arteries adjacent to an airway distal to the respiratory bronchiole were evaluated as previously reported (57). Briefly, arteries were considered fully muscularized when they had a distinct double elastic lamina visible throughout the diameter of the vessel cross section. Arteries were considered partially muscularized when they had a distinct double elastic lamina visible for at least one-half of the diameter. The percentage of vessels with double elastic lamina was calculated as the number of muscularized vessels per total number of vessels counted. In each section, a total of 60–80 vessels were examined using a computer-assisted imaging system (BX51, Olympus, Tokyo, Japan). This analysis was performed for the small vessels with external diameters of 20–70 μm.

Immunofluorescence analysis. We performed immunofluorescence analysis using paraffin-embedded sections as previously described (35). The lungs were rigorously and completely perfused with cold KHB at physiological pressure until the color of the lungs had clearly turned white. They were then fixed in 10% formaldehyde solution for 24 h on a shaker at room temperature. After serial steps of washing and dehydration, the whole lungs were embedded in paraffin, and cross sections (3 μm) were prepared. Paraffin sections were deparaffinized in xylene and thereafter rehydrated and washed in ethanol and

distilled water. Antigen retrieval was carried out by heating the sections in citrate buffer (pH 6.0, Target Retrieval Solution, Dako, Glostrup, Denmark) at 120°C for 5 min. After being blocked with 2% skim milk, sections were incubated overnight at 4°C with the following primary antibodies: nitrotyrosine (1:200, Millipore, Bedford, MA) and actin α-smooth muscle-Cy3 (1:1,000, Sigma-Aldrich). After being washed and blocked with potential endogenous peroxidase, sections were incubated at room temperature for 60 min with secondary antibody, Alexa fluor 488-conjugated donkey anti-rabbit (1:1,000, Molecular Probes, Eugene, OR) for nitrotyrosine. Nuclei were stained with DAPI (ThermoFisher), and immunofluorescence images were obtained using a fluorescence microscope (BZ-9000, KEYENCE, Osaka, Japan). To assess the specificity of nitrotyrosine immunofluorescence, other sections were incubated with nonimmune rabbit IgG instead of anti-nitrotyrosine antibody and were then processed under the same conditions. Exposure time was unified to evaluate nitrotyrosine expression, and the fluorescence intensity of vascular smooth muscle layer, identified by α-smooth muscle staining, was analyzed with ImageJ software. This analysis was performed for the small vessels with external diameters of 20–70 μm; a total of ~15 vessels were examined.

Sugen/hypoxia mouse model. The Sugen/hypoxia (SuHx) mouse model was used as a more severe PH model than the hypoxia-induced PH model (10). Briefly, 11-wk-old male WT mice on a normal chow diet under a 12:12-h light-dark cycle were exposed to hypoxia (10% O_2) for 21 days, and SU5416 (Sigma-Aldrich) was subcutaneously injected at 0, 7, and 14 days. SU5416 was suspended in carboxymethylcellulose sodium containing 0.9% sodium chloride, 0.4% polysorbate 80, and 0.9% benzyl alcohol in deionized water. Hypoxic exposure was performed in an acrylic chamber with a nonrecirculating gas mixture of 10% O_2 and 90% N_2 by adsorption-type oxygen concentrator to use exhaust air as well as hypoxia-induced PH model. All SuHx mice were studied within 1 h of removal from the chamber.

Materials. CTx was obtained from Peptide Institute (Osaka, Japan), and SNP was obtained from Maruishi Seiyaku (Osaka, Japan). All other materials were from Sigma-Aldrich. The ionic composition of KHB was as follows (in mmol/l): 144 Na^+, 5.9 K^+, 1.2 Mg^{2+}, 2.5 Ca^{2+}, 1.2 $H_2PO_4^-$, 24 HCO_3^-, 129.7 Cl^-, and 5.5 glucose.

Statistical analysis. All results are expressed as means ± SE. Comparisons of means between two groups were performed by an unpaired Student's t-test. Comparisons of means among more than four groups were analyzed by one- or two-way-ANOVA followed by Dunnett's or Tukey's test for multiple comparisons. Statistical analysis was performed using GraphPad Prism v. 7.00 (GraphPad Software, La Jolla, CA). Results were considered to be significantly different at values of $P < 0.05$.

RESULTS

Endothelium-dependent relaxation of pulmonary arteries under normoxia. To examine the contribution of EDRFs in pulmonary arteries, we performed isometric tension experiments using first- to second-branch of intrapulmonary arteries. Isolated pulmonary arterial rings from normoxic mice were precontracted with U46619 and subsequently exposed to cumulative concentrations of ACh ($10^{-10}–10^{-5}$ mol/l; Fig. 1A). The endothelium-dependent, ACh-mediated relaxations were resistant to Indo but were highly sensitive to L-NNA, indicating that NO predominantly regulates the tonus of these large proximal intrapulmonary arteries. These results were consistent with dominant roles of NO in endothelium-dependent relaxation of relatively large vessels in the systemic circulation (60). To explore the roles of EDH-mediated responses, we performed isolated perfused lung experiments that enabled us
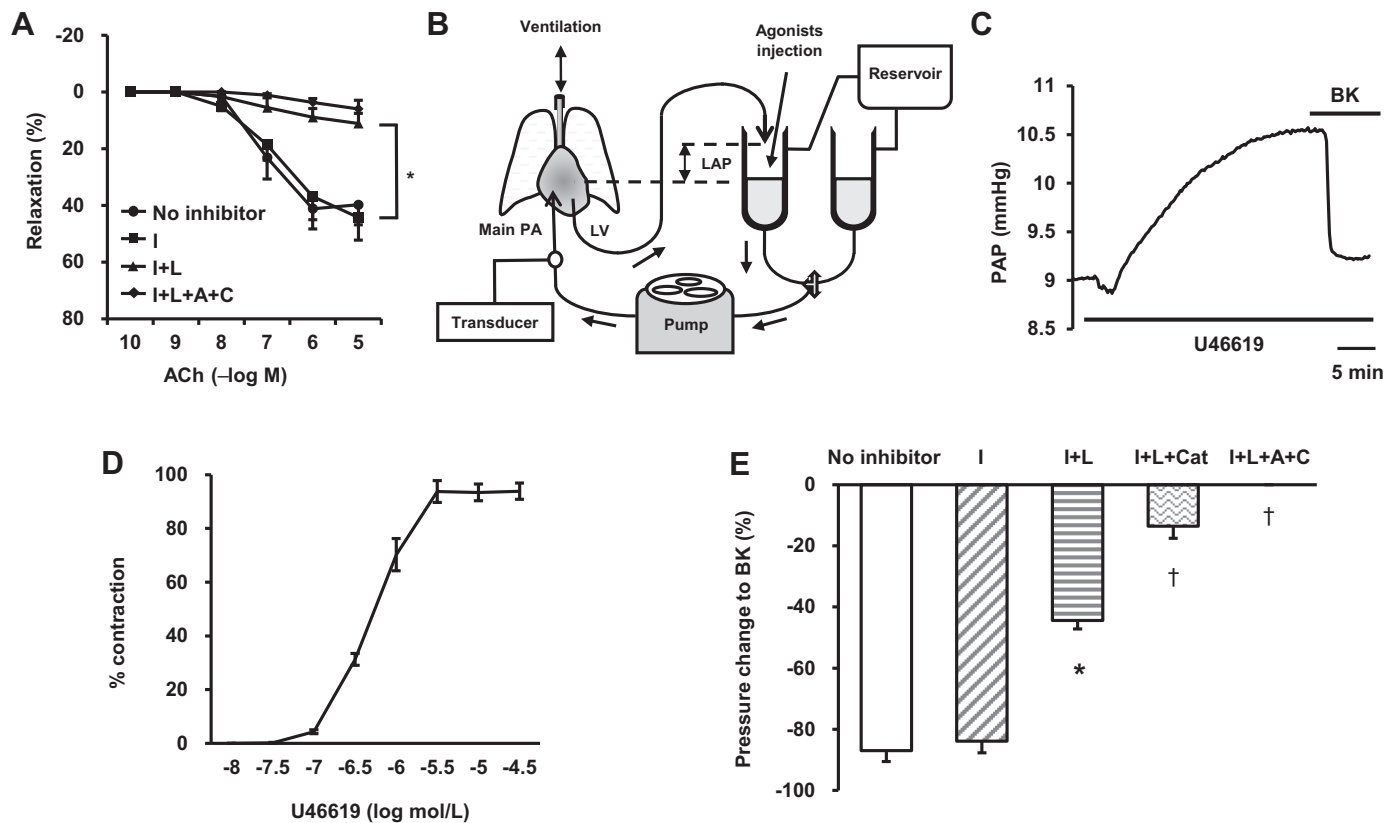
Fig. 1. Endothelium-dependent relaxation of isolated pulmonary arteries under normoxia. *A*: endothelium-dependent relaxation to acetylcholine (ACh; $10^{-10}-10^{-5}$ mol/l) in wild-type (WT) mice under normoxia. Contributions of PGI_2, nitric oxide (NO), and endothelium-dependent hyperpolarization (EDH) were determined by the inhibitory effect of indomethacin (I; 10^{-5} mol/l), N^{ω}-nitro-L-arginine (L; 10^{-4} mol/l), apamin (A; 10^{-6} mol/l), and charybdotoxin (C; 10^{-7} mol/l), respectively. The number of rings examined was as follows: no inhibitor ($n = 7$), indomethacin ($n = 6$), indomethacin + N^{ω}-nitro-L-arginine ($n = 5$), and indomethacine + N^{ω}-nitro-L-arginine + apamin + charybdotoxin ($n = 5$). Results are shown as means ± SE. *$P < 0.05$ vs. indomethacin, analyzed by two-way ANOVA followed by Tukey's test for multiple comparisons. *B*: schematic illustration of the isolated perfused apparatus. LAP, left atrial pressure; LV, left ventricle; PA, pulmonary artery. *C*: representative recording in isolated perfused lung experiments. Relaxations were calculated as percent changes in perfusion pressure from precontracted levels with U46619. We used bradykinin (BK; 10^{-5} mol/l), sodium nitroprusside (SNP; 10^{-5} mol/l), and H_2O_2 (10^{-4} mol/l) as vasodilating agonists. PAP, pulmonary arterial pressure (in mmHg). *D*: dose-response curves to U46619 in WT mice under normoxia. Responses are expressed as percent contraction ($n = 5$). *E*: pressure change to BK in WT mice under normoxia. Inhibitory effects of indomethacin (10^{-5} mol/l), N^{ω}-nitro-L-arginine (10^{-4} mol/l), catalase (Cat; 12,500 U/ml), and the combination of apamin (10^{-6} mol/l) and charybdotoxin (10^{-7} mol/l) were examined ($n = 6$ each). Results are shown as means ± SE. *$P < 0.05$ vs. indomethacin and †$P < 0.05$ vs. indomethacin + N^{ω}-nitro-L-arginine, analyzed by two-way ANOVA followed by Tukey's test for multiple comparisons.

to examine the contributions of EDRFs in the pulmonary microcirculation (4). The schema of the experimental apparatus is shown in Fig. 1*B*. Since relaxations were not induced by vasodilating agonists alone in these models, the lungs were precontracted with U46619 and were then exposed to vasodilating agonists (Fig. 1*C*). To determine the optimal tonus of precontraction, U46619 dose-response curves were obtained (Fig. 1*D*). The concentration of U46619 giving the half-maximal response (EC_{50}: -6.29 ± 0.04 log mol/l) was used to precontract the vessels for subsequent relaxation (46). Almost full relaxations were obtained in response to BK in the absence of any inhibitor in mice under normoxia. Endothelium-dependent relaxation to BK was resistant to Indo, significantly reduced in the presence of L-NNA by ~50% in the presence or absence of Indo, and abolished by the combination of Apa and CTx (Fig. 1*E*), indicating the comparable contributions of NO and EDH to the pulmonary microcirculation under physiological conditions. Importantly, EDH-mediated relaxation was markedly inhibited by catalase (Fig. 1*E*), indicating that endothelium-derived H_2O_2 contributes to EDH-mediated relaxation mainly in the pulmonary microcirculation.

Endothelium-dependent relaxation of pulmonary arteries in response to chronic hypoxia. To assess the roles of EDRFs in the development of PH, we used a chronic hypoxia model as a well-established model of PH (57). In mice exposed to chronic hypoxia compared with those under normoxia, endothelium-dependent relaxation to BK in the absence of any inhibitor was significantly reduced, whereas BK-mediated relaxation in the presence of Indo was enhanced compared with those without Indo (Fig. 2*A*). These results indicate that vasoconstrictor PGs might be increased by chronic hypoxia. Intriguingly, L-NNA markedly inhibited BK-mediated relaxation in lungs exposed to chronic hypoxia compared with normoxia, suggesting that NO plays a compensatory role for reduced EDH-mediated responses under chronic hypoxia (Fig. 2, *A* and *B*). In contrast, endothelium- independent relaxations to SNP and to exogenous H_2O_2 were comparable between normoxic and hypoxic mice (Fig. 2, *C* and *D*).

Transition of the role in BK-mediated relaxation of the pulmonary microcirculation from EDH to NO during hypoxia. Next, we examined isolated perfused lungs using the mice exposed to hypoxia for 1, 2, 7, and 14 days to clarify when
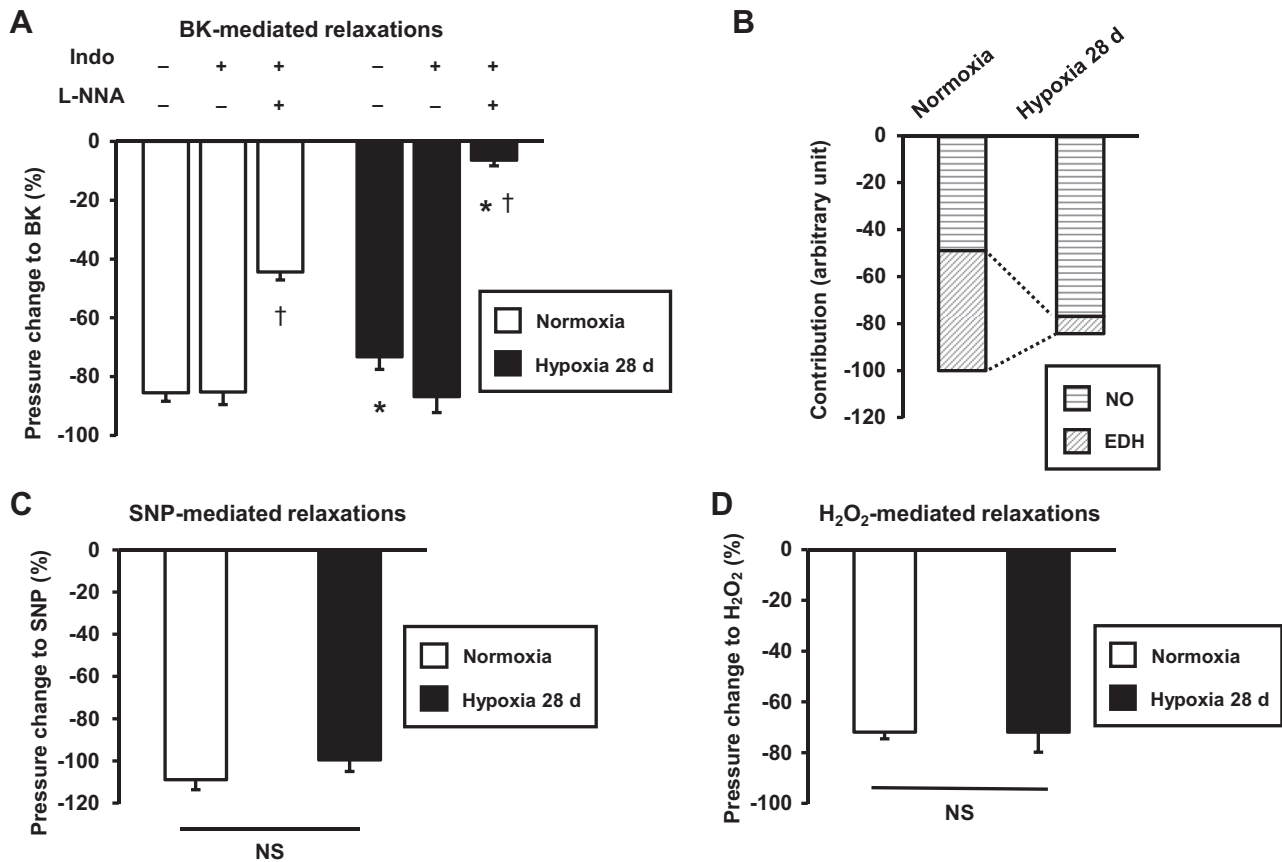
Fig. 2. Endothelium-dependent relaxation in the pulmonary circulation after chronic hypoxia. *A*: endothelium-dependent relaxation to bradykinin (BK) in the absence or presence of indomethacin (Indo; 10^{-5} mol/l) and/or N^{ω}-nitro-L-arginine (L-NNA; 10^{-4} mol/l) in lungs from normoxic mice and 28-day hypoxic mice ($n = 6$ each). Results are shown as means ± SE. *$P < 0.05$ vs. normoxia and †$P < 0.05$ vs. Indo in each group, analyzed by two-way ANOVA followed by Tukey's test for multiple comparisons. *B*: changes in contributions of nitric oxide (NO) and endothelium-dependent hyperpolarization (EDH) in BK-mediated relaxation between normoxic and hypoxic mice for 28 days. Contributions were calculated as relative degree to the relaxation in "no inhibitor" in mice under normoxia. *C*: endothelium-independent relaxation to sodium nitroprusside (SNP; 10^{-5} mol/l, $n = 6$ each). Results are shown as means ± SE and were analyzed by unpaired *t*-test. *D*: endothelium-independent relaxation to exogenous H_2O_2 (10^{-4} mol/l) in the presence of Indo and L-NNA ($n = 6$ each). Results are shown as means ± SE and were analyzed by unpaired *t*-test.

hypoxia causes the transition from EDH to NO as a main mediator in BK-induced relaxation. Baseline perfusion pressure was comparable between normoxic and hypoxic mice (Fig. 3*A*). In contrast, basal pulmonary vascular resistance was significantly increased at *day 2* of hypoxia compared with normoxia (Fig. 3*B*). The discrepancy between baseline perfusion pressure and basal pulmonary vascular resistance could be attributed to the adjustment of the flow rate by body weight, as hypoxic exposure significantly reduced body weight (data not shown). Interestingly, although endothelium-dependent relaxation to BK was significantly reduced at *day 1* of hypoxia compared with normoxia and was then unchanged until *day 28* (Fig. 3*C*), EDH-mediated relaxation was significantly reduced as early as *day 2* of hypoxia (Fig. 3*D*), suggesting that the transition from EDH to NO during hypoxia occurred at *day 2*.

Mechanisms of the compensatory role of NO for reduced EDH in endothelium-dependent relaxation of the pulmonary microcirculation during hypoxia. Western blot analyses using whole lung lysates showed that total eNOS expression was increased in the lungs at *day 28* of hypoxia (Fig. 4, *A* and *C*). In the lungs from normoxic mice, eNOS phosphorylation was evident at Thr[495] but to a lesser extent at Ser[1177] (Fig. 4*A*). Hypoxia significantly dephosphorylated eNOS at Thr[495] and

phosphorylated at Ser[1177] at *day 28* (Fig. 4, *A*, *D*, and *E*). Similarly, hypoxia significantly pVASP at Ser[239] at *days 2* and *28* (Fig. 4, *A* and *F*). Furthermore, hypoxia significantly downregulated Cav-1, which negatively regulates eNOS activity by binding to the eNOS oxygenase domain (25), at *days 2* and *28* (Fig. 4, *A* and *G*). Immunoprecipitation of eNOS with Cav-1 showed that hypoxia had no significant effect on the eNOS: Cav-1 complex (Fig. 4, *B* and *H*). Taken together, these results suggest that upregulation and activation of eNOS associated with downregulation of Cav-1 enhanced the compensatory role of NO for reduced EDH, a consistent finding with the isolated perfused lung experiments.

Pulmonary artery remodeling and development of PH after hypoxic exposure. Elastica-Masson staining showed muscularization of distal pulmonary arteries, which was defined as nonmuscularized, partially muscularized, and fully muscularized (Fig. 5*A*). As expected, the extent of muscularization was significantly accelerated at *day 28* of hypoxia (Fig. 5, *B* and *C*), but morphological changes were not noted until *day 2* of hypoxia. Consistent with the muscularization of distal pulmonary arteries, only mice exposed to hypoxia for 28 days exhibited marked increases in RVSP (Fig. 5*D*) but not in RVEDP (Fig. 5*E*). These results indicate that, during the development of hypoxia-induced
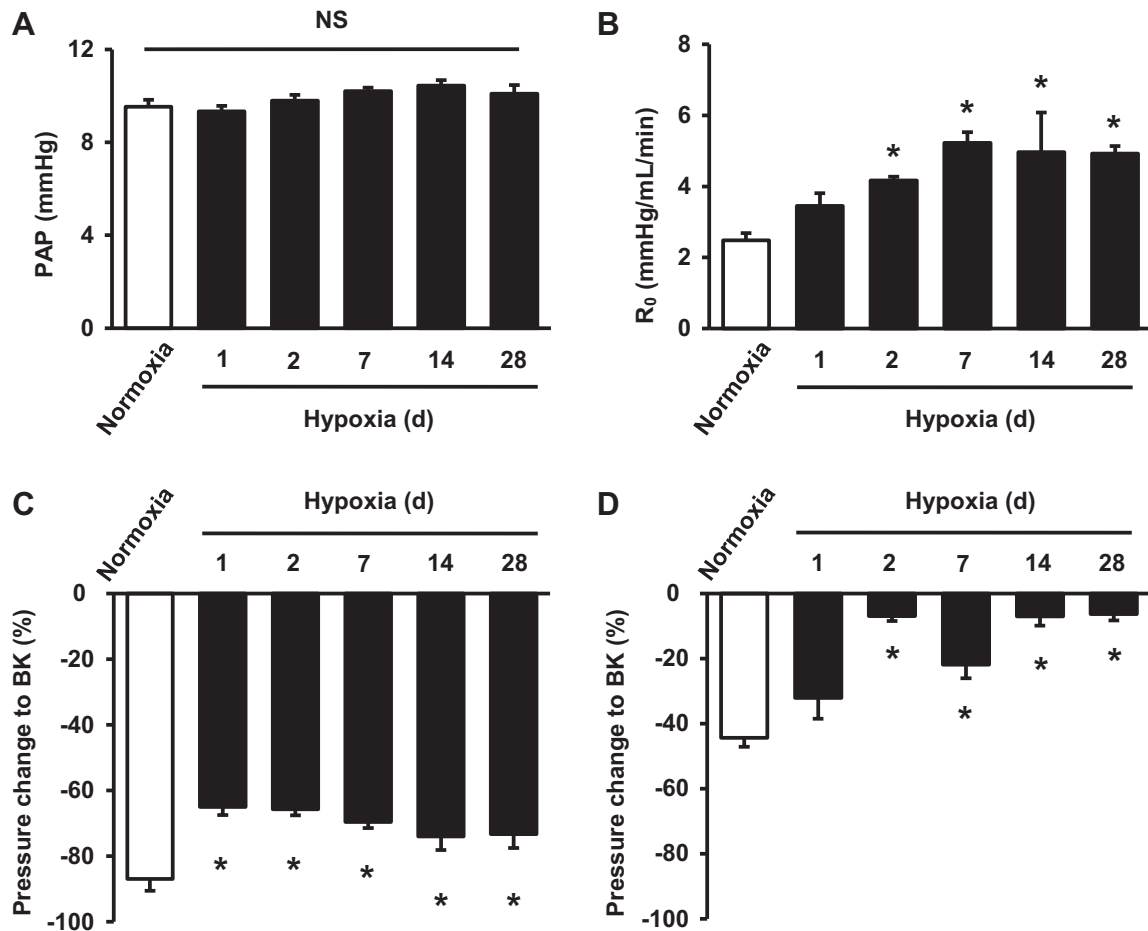
Fig. 3. Time course of endothelium-dependent relaxation in the pulmonary circulation in response to chronic hypoxia. *A*: baseline perfusion pressures in normoxic and hypoxic mice. PAP, pulmonary arterial pressure. *B*: basal pulmonary vascular resistance (R_0) in normoxic and hypoxic mice ($n = 6$ each). *C*: endothelium-dependent relaxation to bradykinin (BK) in the absence of inhibitor in normoxic and hypoxic mice ($n = 6$ each). *D*: endothelium-dependent relaxation to BK in the presence of indomethacin and N^ω-nitro-L-arginine (endothelium-dependent hyperpolarization-type relaxation, $n = 6$ each). All results are shown as means ± SE. *$P < 0.05$ vs. normoxia, analyzed by one-way ANOVA followed by Dunnett's test for multiple comparisons. NS, not significant.

PH, impairment of EDH-mediated relaxation precedes morphological changes of the pulmonary artery.

Increased nitrotyrosine levels in vascular smooth muscle after hypoxic exposure. We next hypothesized that the transition from EDH to NO in BK-mediated relaxation might be involved in vascular smooth muscle remodeling in response to chronic hypoxia. Immunofluorescence showed the ubiquitous presence of 3-nitrotyrosine (3-NT) in lung tissues of both normoxia and hypoxia (Fig. 6*A*). In contrast, the lung tissues exposed to chronic hypoxia slightly but significantly exhibited a higher level of 3-NT in the vascular smooth muscle layer than in the lungs under normoxia (Fig. 6, *A* and *B*). These results suggest that chronic hypoxia-induced NO upregulation results in nitrosylation in pulmonary artery vascular smooth muscle, implying that nitrosylation in vascular smooth muscle might be involved in pulmonary artery remodeling after chronic hypoxia.

Endothelium-dependent relaxation in the SuHx mouse model. To evaluate vascular reactivity in the severe PH model, we performed isolated perfused lung experiments using the SuHx mouse model, which is an established model of more severe PH (10). Weekly SU5416 injections, during hypoxia for 3 wk, significantly elevated RVSP but not RVEDP compared with normoxia (Fig. 7, *A* and *B*). RVSP tended to be elevated

more in SuHx than in chronic hypoxia (SuHx: 39.4 ± 4.2 mmHg vs. chronic hypoxia: 36.6 ± 2.0 mmHg, $P = 0.57$). SuHx exhibited higher baseline perfusion pressure and basal pulmonary vascular resistance compared with normoxia (Fig. 7, *C* and *D*). In line with the results of the chronic hypoxia model, endothelium-dependent relaxation to BK tended to be reduced in SuHx compared with normoxia ($P = 0.07$; Fig. 7*E*), and Indo significantly improved but additive L-NNA markedly diminished BK-mediated relaxation in SuHx compared with normoxia (Fig. 7*E*), indicating that SuHx also induces the transition from EDH to NO in BK-mediated relaxation as well as chronic hypoxia (Fig. 7*F*).

DISCUSSION

The major findings of the present study are as follows. First, EDH plays an important role in endothelium-dependent relaxation in the pulmonary microcirculation, in addition to NO, under normoxia in mice. Second, endothelium-derived H_2O_2 plays an important role in EDH-mediated relaxation in the pulmonary microcirculation under normoxia. Third, hypoxia impairs the role of EDH in endothelium-dependent relaxation as early as 2 days with a resultant compensatory role of NO.
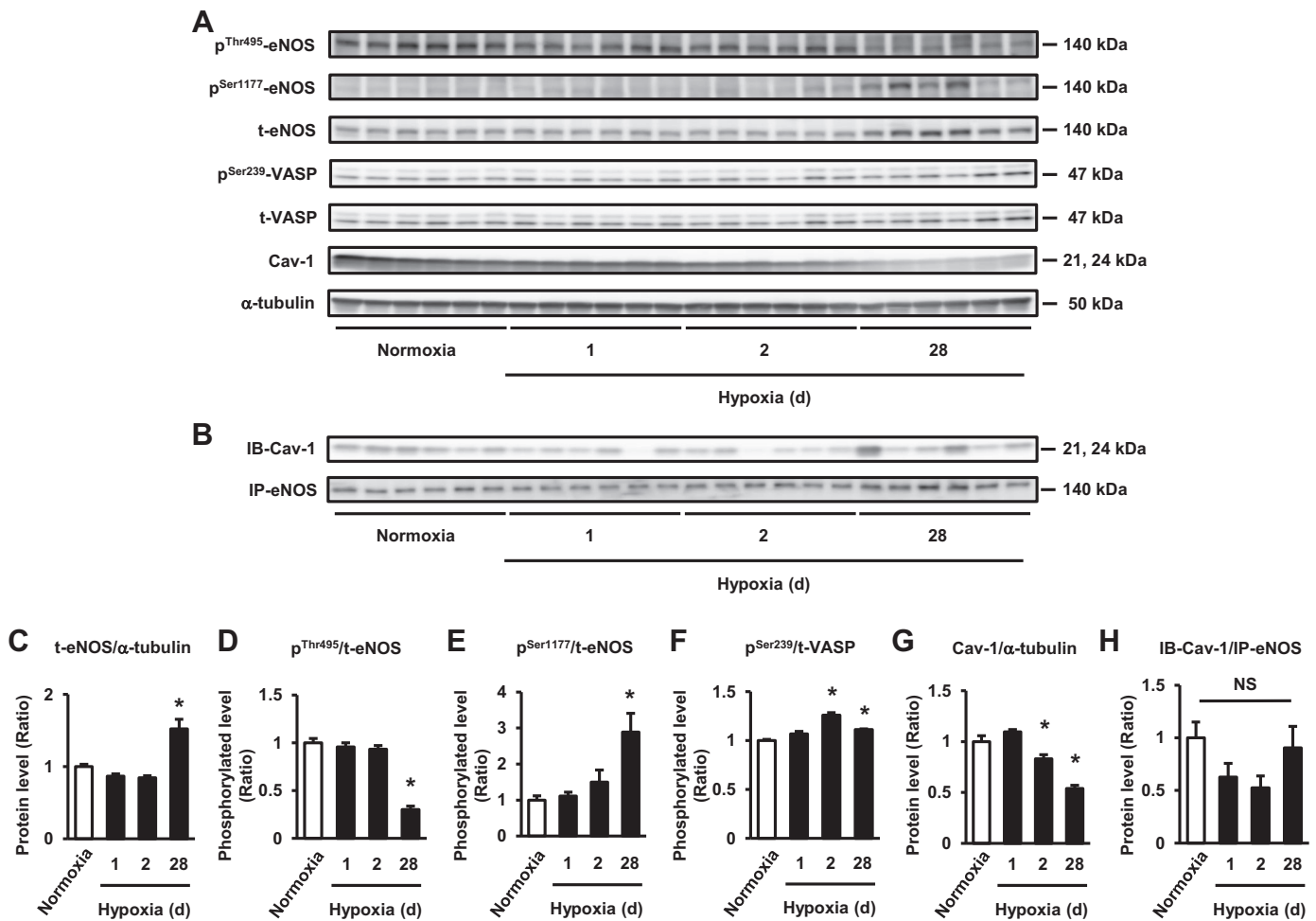
Fig. 4. Effects of hypoxia on nitric oxide (NO)-mediated signaling in normoxic and hypoxic mice. A: representative Western blots for phosphorylated (p)Thr^{495}-endothelial NO synthase (eNOS), pSer^{1177}-eNOS, total (t-)eNOS, pSer^{239}-vasodilator-stimulated phosphoprotein (VASP), total (t-)VASP, caveolin-1 (Cav-1), and α-tubulin (for loading control) using whole lung lysates from mice under normoxia and hypoxia (for 1, 2, and 28 days, $n = 6$ each). All phosphorylated proteins were detected before the total proteins. B: representative Western blots showing the association of Cav-1 with eNOS immunoprecipitated from whole lung lysates of normoxic and hypoxic mice (for 1, 2, and 28 days, $n = 6$ each). C–H: each bar graph shows expressions or phosphorylated levels of each protein. Protein expressions were normalized to α-tubulin, and phosphorylated levels were normalized to total protein expressions. Whole lung lysates were applied in the same order in all blots. Results are shown as means ± SE of the relative value with normoxia as 1. *$P < 0.05$ vs. normoxia, analyzed by one-way ANOVA followed by Dunnett's test for multiple comparisons. IB, immunoblot; IP, immunoprecipitation.

Fourth, this compensatory role of NO is mediated, at least in part, by the enhanced expression and activation of eNOS associated with decreased expression of Cav-1 before the development of hypoxia-induced PH. Fifth, hypoxia induces nitrosylation, especially in pulmonary artery vascular smooth muscle. Sixth, NO-mediated relaxation compensates for impaired EDH-mediated relaxation in the SuHx PH model as in the hypoxia-induced PH model. To the best of our knowledge, this is the first study that demonstrates that EDH factor/H$_2$O$_2$ plays an important role in the pulmonary microcirculation in addition to NO and that the impairment of the role of EDH could be one of the initial processes of hypoxia-induced PH.

Contributions of EDH and other EDRFs in the pulmonary circulation under normoxic conditions. In systemic vessels, there is a general consensus on the converse contribution of NO and EDH in a vessel size-dependent manner, as the contribution of EDH increases while that of NO decreases as vessel size becomes smaller (59). Indeed, we have previously demonstrated the crucial roles of EDH in regulating the tonus

of resistance arteries, adjusting organ perfusion and blood pressure, and modulating coronary autoregulation and metabolic dilatation (64, 73, 74). The present study demonstrates that EDH contributes to endothelium-dependent relaxation of pulmonary arteries in addition to NO under normoxic conditions. Importantly, in the present study, not only the combination of Apa and CTx but also catalase significantly inhibited non-PG- and non-NO-mediated relaxation, suggesting the important role of endothelium-derived H$_2$O$_2$ as one of EDH factors in pulmonary circulation. NO and H$_2$O$_2$ modulate each other in a complex manner; H$_2$O$_2$ not only activates eNOS through the phosphatidylinositol 3-kinase pathway (65) but also suppresses the enzyme in a redox-dependent manner via PKG modification (8). Also, NO desensitizes blood vessels to H$_2$O$_2$-induced vasodilatation, and, in turn, pharmacological inhibition of sGC sensitizes blood vessels to H$_2$O$_2$-induced vasodilatation in mice (8, 29). There appears to be a physiological balance between NO and EDH/H$_2$O$_2$ under physiological conditions, and previous studies have shown that relative
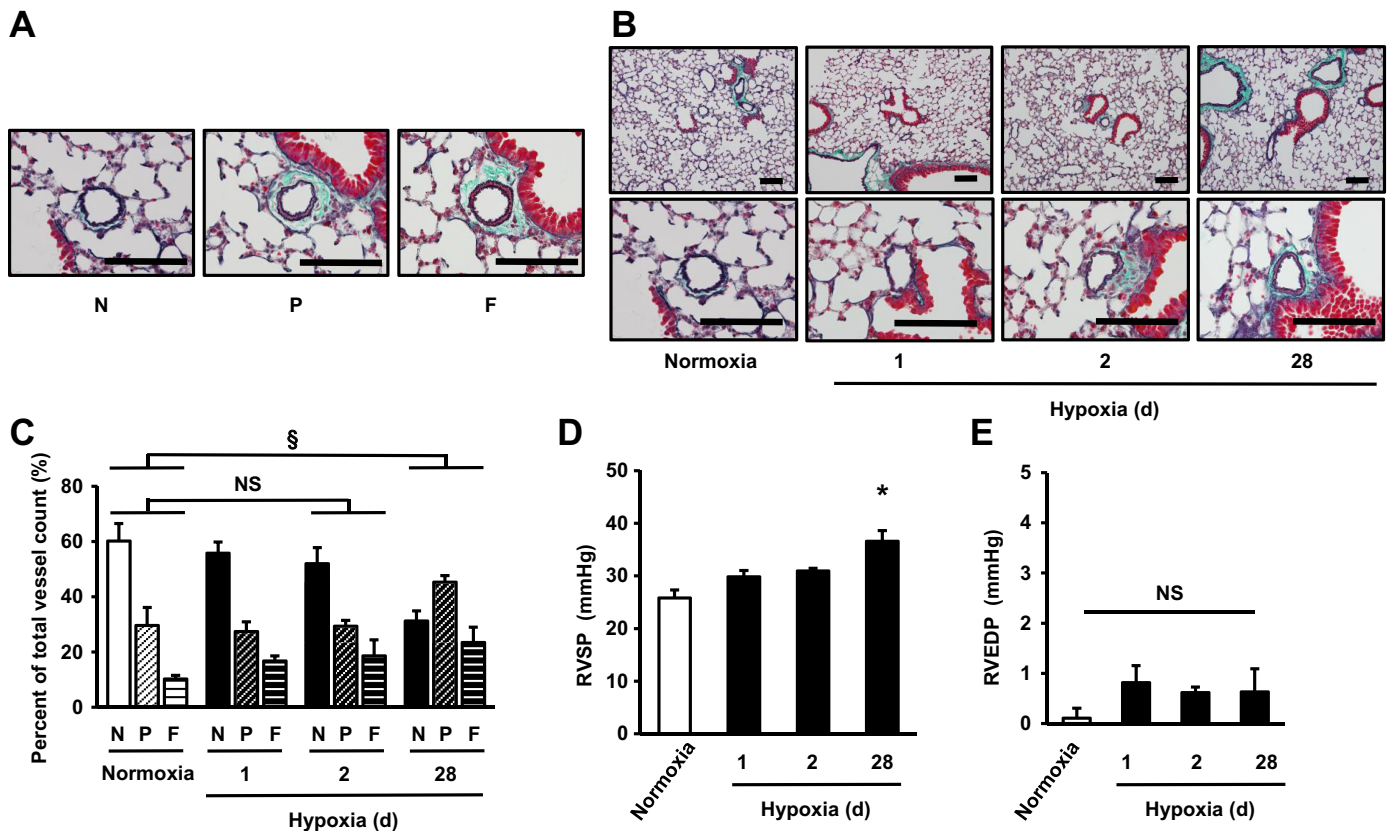
Fig. 5. Morphological and hemodynamic changes in response to hypoxia in mice. *A*: representative elastica-Masson (EM) stainings of distal pulmonary arteries. N, nonmuscularized vessels; P, partially muscularized vessels; F, fully muscularized vessels. Scale bars = 100 μm. *B*: representative EM stainings of distal pulmonary arteries in normoxic and hypoxic (for 1, 2, and 28 days) mice. Scale bars = 100 μm. *C*: muscularization of distal pulmonary arteries with a diameter of 20–70 μm in normoxic and hypoxic mice ($n = 3$ each). In each section, 60–80 vessels (20- to 70-μm external diameters) were examined. Percentages of muscularized vessels were calculated as the number of muscularized vessels per total number of vessels counted. Results are shown as means ± SE. §$P < 0.05$, analyzed by one-way ANOVA followed by Dunnett's test for multiple comparisons. *D* and *E*: right ventricular systolic pressure (RVSP; *D*) and right ventricular end-diastolic pressure (RVEDP; *E*) in normoxic and hypoxic mice measured by right heart catheterization ($n = 7$ each). Results are shown as means ± SE. *$P < 0.05$ vs. normoxia, analyzed by one-way ANOVA followed by Dunnett's test for multiple comparisons. NS, not significant.

contributions of them to endothelium dependent vasodilatation vary depending on the vasculature, species, and experimental conditions examined (19, 59). We have previously reported that Cav-1 is one of the key factors for regulating this physiological balance between NO and EDH by binding to eNOS in systemic arteries of male mice (28, 50). In addition, both SK_{Ca} and IK_{Ca} channels in endothelial cells are involved in EDH-mediated relaxation (13, 27), and BK_{Ca} channel activation leads to vascular smooth muscle hyperpolarization in response to H_2O_2 (7, 33). In the present study, both catalase-sensitive mediator and Apa/CTx-sensitive mediator contributed to EDH-mediated relaxation under physiological conditions. The detailed mechanisms of the contributions of NO, H_2O_2, SK_{Ca}, IK_{Ca}, and BK_{Ca} to the pulmonary circulation remain to be fully elucidated in future studies. From another viewpoint, in the pulmonary circulation, NO has an approximately one-half contribution to BK-mediated relaxation even in resistance vessels, which may underlie the difference in arterial functions between the systemic and pulmonary circulations. Indeed, vascular responses to acute hypoxia are quite different between coronary and pulmonary arteries (12, 17). This viewpoint may provide a clue to modulate vascular responses under hypoxia.

Effects of chronic hypoxia on endothelium-dependent relaxation in the pulmonary circulation. Chronic hypoxia impairs endothelium-dependent relaxation and directly affects vascular smooth muscle cells by altering substrate bioavailability for NOS (16, 71). On the other hand, acute hypoxia does not affect BK-mediated relaxation of either male or female porcine pulmonary arteries or male guinea pig basilar arteries (17, 54). In the present study, BK-mediated relaxation was impaired as early as *day 1* of hypoxia, whereas they remained unchanged until *day 28*. Importantly, hypoxia for 2 days caused a transition from EDH to NO in BK-mediated relaxation, indicating the compensatory role of NO for reduced EDH in response to hypoxia. Furthermore, consistent with these results, exposure to chronic hypoxia caused an ~1.5-fold increase in eNOS expression, enhanced phosphorylation at stimulatory Ser^{1177} and decreased phosphorylation at inhibitory Thr^{495}. Similarly, phosphorylation of VASP at Ser^{239}, a marker of PKG activity, was also significantly enhanced at *day 2* of hypoxia. Interestingly, Cav-1 expression was significantly reduced only after 2 days of hypoxia, although eNOS:Cav-1 complexes were unaltered. Cav-1 hinders electron transfer and inhibits NO generation by binding to eNOS and forming eNOS:Cav-1 complex (25, 50). Thus, the reduced levels of
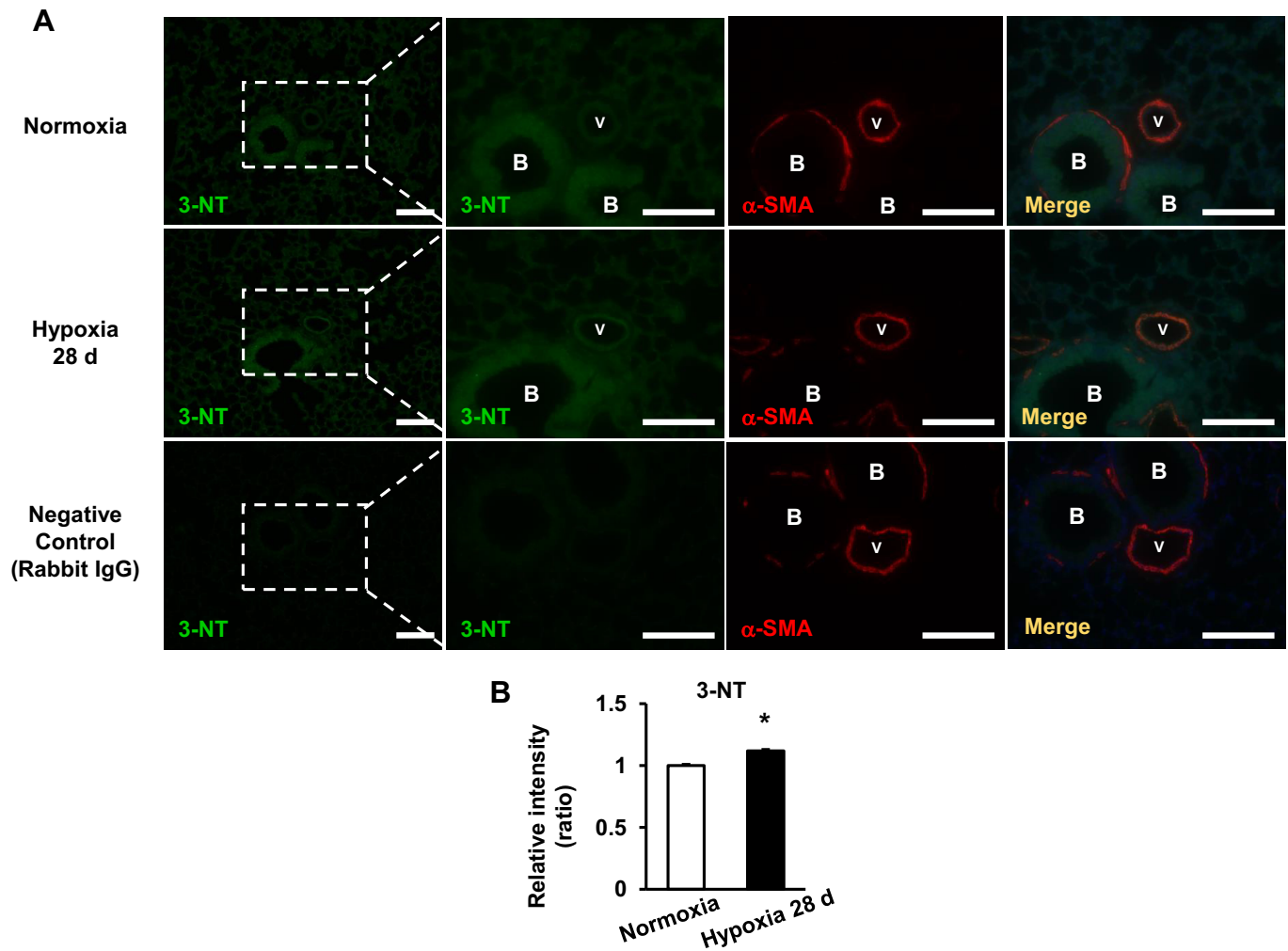
A

B

Fig. 6. Nitrotyrosine (3-NT) expression in lungs from normoxic and chronic hypoxic mice. *A*: representative immunofluorescence for 3-NT; green), α-smooth muscle actin (α-SMA; red), and DAPI (blue) of lung sections from normoxic and chronic hypoxic mice. To assess the specificity of 3-NT immunofluorescence, nonimmune rabbit IgG was used in place of anti-3-NT antibody. Scale bars = 100 μm. *B*: analysis of immunofluorescence intensity in the pulmonary artery smooth muscle layer of lung sections from normoxic and chronic hypoxic mice using ImageJ software. This analysis was performed for ~15 small vessels with external diameters of 20–70 μm from each group (*n* = 3), and results are shown as means ± SE of relative intensity with normoxia as 1. *$P < 0.05$ vs. normoxia, analyzed by unpaired *t*-test.

Cav-1 in response to hypoxia may cause eNOS/VASP activation, triggering the transition from EDH to NO in endothelium-dependent relaxation of pulmonary arteries. Although the mechanisms of the comparable contributions of NO and EDH under physiological conditions also remain unclear, the interaction between eNOS and Cav-1 is likely to be involved in hypoxia-induced functional alterations in BK-mediated relaxation in pulmonary arteries as well as systemic resistance vessels. In the SuHx model, NO also played a dominant role in BK-mediated relaxation as well as the hypoxia-induced PH model, although hypoxia itself may be responsible for the compensatory increase of NO. Taken together, it is also conceivable that Cav-1 can be a therapeutic target for PH to maintain the physiological balance between NO and EDH (28).

Hypoxia-induced PH in mice is an established model, and the phenotypes of PH, such as a rise in RVSP, pulmonary vascular remodeling, and RV hypertrophy, appear after 3–4 wk of hypoxia (57). In the present study, baseline pulmonary perfusion pressure in isolated perfused lung was unchanged

after chronic hypoxia, an inconsistent finding with previous reports (1, 18). We consider that this discrepancy between the present study and previous reports is based on the fact that we adjusted perfusion flow rate by body weight in the present study, since hypoxia caused a significant body weight loss and induced a relatively low perfusion flow in hypoxic mice. Indeed, 4 wk of hypoxia caused not only PH phenotypes in mice but also significantly increased pulmonary vascular resistance in isolated perfused lung, indicating the integrity of the hypoxia-induced PH model in the present study. In addition, we consider that baseline pulmonary perfusion pressure was appropriately evaluated, since it reflected the severity of PH in the SuHx model.

Effects of hypoxia-induced compensatory NO upregulation on pulmonary artery vascular smooth muscle. NO regulates vascular tonus via the sGC/cGMP/PKG pathway (70). In the pulmonary circulation, it has been previously reported that reduced NO bioavailability is involved in the pathogenesis of PH (15, 26, 53). Moreover, the importance of the NO pathway in the pulmonary circulation is supported by the effectiveness
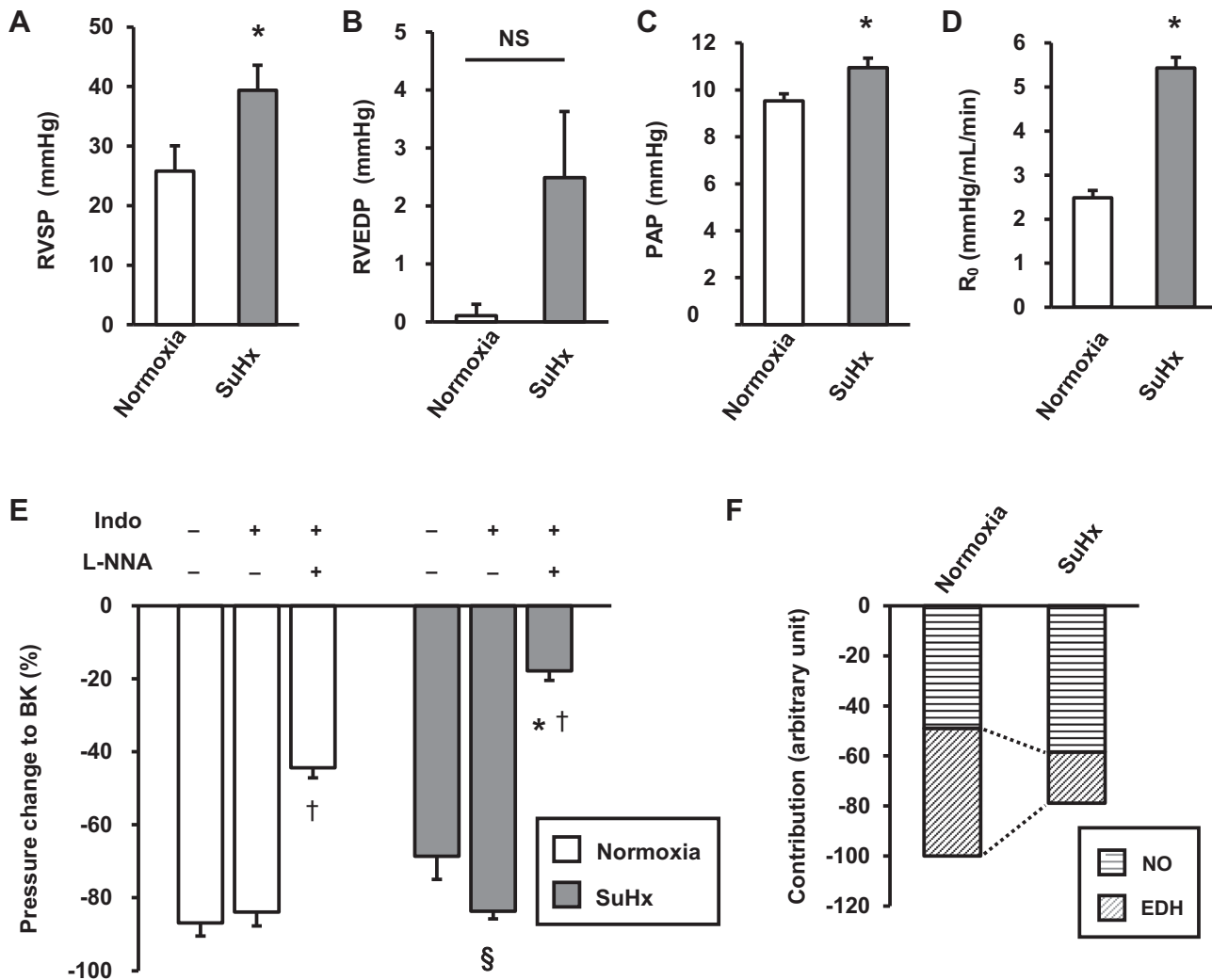
Fig. 7. Endothelium-dependent relaxation in the Sugen/hypoxia (SuHx) mouse model. A and B: right ventricular systolic pressure (RVSP; A) and right ventricular end-diastolic pressure (RVEDP; B) measured by right heart catheterization in normoxic and SuHx mice ($n = 7$ each). Results are shown as means ± SE. *$P < 0.05$ vs. normoxia, analyzed by an unpaired t-test. C: baseline perfusion pressures in normoxic and SuHx mice. Results are shown as means ± SE. PAP, pulmonary arterial pressure. *$P < 0.05$ vs. normoxia, analyzed by unpaired t-test. D: basal pulmonary vascular resistance (R_0) in normoxic and SuHx mice ($n = 6$ each). Results are shown as means ± SE and were analyzed by an unpaired t-test. E: endothelium-dependent relaxation to BK in the absence or presence of indomethacin (Indo; 10^{-5} mol/l) and/or N^{ω}-nitro-L-arginine (L-NNA; 10^{-4} mol/l) in lungs from normoxic and SuHx mice ($n = 6$ each). Results are shown as means ± SE. *$P < 0.05$ vs. normoxia, †$P < 0.05$ vs. Indo in each group, and §$P < 0.05$ vs. no inhibitor in the SuHx group, analyzed by two-way ANOVA followed by Tukey's test for multiple comparisons. F: changes in contributions of nitric oxide (NO) and endothelium-dependent hyperpolarization (EDH) to BK-mediated relaxation between normoxic and SuHx mice. Contributions were calculated as relative degree to relaxation in "no inhibitor" in mice under normoxia.

of inhaled NO (30, 39), sGC modulators (23, 24), and selective PDE5 inhibitors (20) in PAH patients. However, it has been controversial whether the pathogenesis of PAH is attributed to the reduced bioavailability of NO. Although it has been reported that reduced NO bioavailability leads to the onset of PH (15, 26, 53), there also is opposite evidence that upregulated eNOS or enhanced eNOS-derived NO production could lead to the development of PH in animals and humans (42, 72, 77). From the latter viewpoint, it is conceivable that excessive NO might be involved in the pathogenesis of PH.

NO reacts with superoxide anions at an extremely fast rate and forms peroxynitrite, which causes protein modification via tyrosine nitration (55). It has been previously reported that chronic exposure to hypoxia increases the production of superoxide anions through NADPH oxidase in male mice (41, 49).

In the present study, hypoxia diminished EDH-mediated relaxation and induced compensatory NO upregulation with increased expression and activation of eNOS. All together, the present study suggests that the hypoxia-induced transition of vasodilators from EDH to NO resulted in peroxynitrite formation followed by nitrosative stress in pulmonary arteries. Indeed, the present immunofluorescence data showed that 3-NT is ubiquitously present, especially in the vascular smooth muscle layer of hypoxic mice, providing evidence that enhanced NO production induced by chronic hypoxia causes nitrosative stress in pulmonary artery vascular smooth muscle. Although it remains unclear whether nitrosylation of vascular smooth muscle causes vascular remodeling, a previous report (6) has shown that 3-NT expression is ubiquitously present in the lungs of patients with severe PH but not in those from

controls. Similarly, inhaled NO increases both superoxide and peroxynitrite, resulting in elevated pulmonary vascular resistance and the onset of rebound PH (51). In contrast, Sheak et al. (58) recently reported that chronic hypoxia does not alter the expression of 3-NT in neonatal rats regardless of enhanced NO. The discrepancy between that report and the present study may be attributed to the different experimental methods to evaluate 3-NT: Western blot analysis with whole lung homogenates from neonatal rats (58) versus immunofluorescence in the present study. It is possible that the whole lung evaluation may underestimate the increased expression of 3-NT in the vascular smooth muscle layer of chronic hypoxic lungs. Thus, although it is inconclusive whether nitrosylation in vascular smooth muscle directly causes vascular remodeling in the clinical situation, it may be an effective treatment to reduce nitrosative stress for PH patients. It should be mentioned that SNP-mediated relaxation was unaltered in response to chronic hypoxia in the present study, indicating preserved function of the pathway downstream of NO after chronic hypoxia. These results are consistent with the clinical evidence that inhaled NO, sGC modulators, and selective PDE5 inhibitors are effective in reducing pulmonary artery pressure in PAH patients (20, 23, 24, 30, 39).

Study limitations. Several limitations should be mentioned for the present study. First, although catalase-sensitive relaxation generally indicates H_2O_2-mediated relaxation, catalase may not be a specific scavenger of H_2O_2 (22). In systemic blood vessels, we have previously demonstrated that endothelium-derived H_2O_2 plays a major role as an EDH in animals and humans using dichlorodihydrofluorescein diacetate and electron spin resonance (45, 59, 64). In contrast, several factors other than H_2O_2 have been proposed as a candidate of EDH in systemic blood vessels (21, 40), and several K^+ channels may also be involved in the development of PAH (2, 5, 52, 71). Further studies are needed to address this point. Second, it remains to be elucidated whether changes in Cav-1 expression contribute to the onset of PH. It has been reported that mutant Cav-1-F92A increases NO bioavailability but does not cause PH as in the case of male Cav-1 knockout mice (36). On the other hand, it has also been reported that Cav-1 is downregulated in PAH patients (76) and that endothelial Cav-1 exerts a protective role against spontaneous development of PH in male mice (47). Third, although PAH is a disease with high prevalence in females (66), we used only male mice in the present study. Regarding the high prevalence of females, sex hormones, especially estrogen, are considered to be one of the possible contributors to the pathogenesis of PAH (63). Estrogen has positive roles in the vascular functions of pulmonary arteries through eNOS upregulation and activation in addition to enhancing PGI_2 release and endothelin-1 downregulation, leading to relaxation of pulmonary arteries and inhibition of hypoxic pulmonary vasoconstriction (37). Thus, female sex may exhibit better pulmonary artery reactivity than male sex. However, despite the positive effects of estrogen on pulmonary vessels, the opposite evidence has also been demonstrated, i.e., that exogenous estrogen treatments promote the onset of PAH (63); these two-sided effects of estrogen are known as the "estrogen paradox" (68). Further studies are warranted to investigate the sex difference in endothelium-dependent relaxation in the pulmonary circulation. Fourth, the discrepancy between the slight rise in RVSP and the marked increase in

basal pulmonary vascular resistance could be attributed to the development of RV failure, which was not evaluated in the present isolated perfused lung model. However, according to the previous report, RV contractility is preserved after 21 days of hypoxia in WT mice (11).

Conclusions. In the present study, we were able to demonstrate that EDH plays an important role in pulmonary microcirculation in addition to NO under normoxic conditions and that impaired EDH-mediated relaxation and subsequent nitrosative stress may be potential triggers of the onset of PH.

DISCLOSURES

No conflicts of interest, financial or otherwise, are declared by the authors.

AUTHOR CONTRIBUTIONS

S.T., T.S., S.G., H. Saito, Y.I., A.I., S.K., and H. Shimokawa conceived and designed research; S.T. and S.S. performed experiments; S.T. analyzed data; S.T., T.S., S.G., H. Saito, Y.I., A.I., S.K., and H. Shimokawa interpreted results of experiments; S.T., T.S., S.G., H. Saito, and H. Shimokawa prepared figures; S.T., T.S., S.G., and H. Shimokawa drafted manuscript; S.T., T.S., S.G., and H. Shimokawa edited and revised manuscript; S.T., T.S., S.G., H. Saito, Y.I., A.I., S.K., S.S., and H. Shimokawa approved final version of manuscript.

REFERENCES

1. **Adnot S, Raffestin B, Eddahibi S, Braquet P, Chabrier PE.** Loss of endothelium-dependent relaxant activity in the pulmonary circulation of rats exposed to chronic hypoxia. *J Clin Invest* 87: 155–162, 1991. doi:10.1172/JCI114965.

2. **Antigny F, Hautefort A, Meloche J, Belacel-Ouari M, Manoury B, Rucker-Martin C, Péchoux C, Potus F, Nadeau V, Tremblay E, Ruffenach G, Bourgeois A, Dorfmüller P, Breuils-Bonnet S, Fadel E, Ranchoux B, Jourdon P, Girerd B, Montani D, Provencher S, Bonnet S, Simonneau G, Humbert M, Perros F.** Potassium channel subfamily K member 3 (KCNK3) contributes to the development of pulmonary arterial hypertension. *Circulation* 133: 1371–1385, 2016. doi:10.1161/CIRCULATIONAHA.115.020951.

3. **Barst RJ, Rubin LJ, Long WA, McGoon MD, Rich S, Badesch DB, Groves BM, Tapson VF, Bourge RC, Brundage BH, Koerner SK, Langleben D, Keller CA, Murali S, Uretsky BF, Clayton LM, Jöbsis MM, Blackburn SD Jr, Shortino D, Crow JW; Primary Pulmonary Hypertension Study Group.** A comparison of continuous intravenous epoprostenol (prostacyclin) with conventional therapy for primary pulmonary hypertension. *N Engl J Med* 334: 296–301, 1996. doi:10.1056/NEJM199602013340504.

4. **Bhattacharya J, Gropper MA, Staub NC.** Interstitial fluid pressure gradient measured by micropuncture in excised dog lung. *J Appl Physiol Respir Environ Exerc Physiol* 56: 271–277, 1984.

5. **Boucherat O, Chabot S, Antigny F, Perros F, Provencher S, Bonnet S.** Potassium channels in pulmonary arterial hypertension. *Eur Respir J* 46: 1167–1177, 2015. doi:10.1183/13993003.00798-2015.

6. **Bowers R, Cool C, Murphy RC, Tuder RM, Hopken MW, Flores SC, Voelkel NF.** Oxidative stress in severe pulmonary hypertension. *Am J Respir Crit Care Med* 169: 764–769, 2004. doi:10.1164/rccm.200301-147OC.

7. **Burgoyne JR, Madhani M, Cuello F, Charles RL, Brennan JP, Schröder E, Browning DD, Eaton P.** Cysteine redox sensor in PKGIa

enables oxidant-induced activation. *Science* 317: 1393–1397, 2007. doi:10.1126/science.1144318.

8. **Burgoyne JR, Prysyazhna O, Rudyk O, Eaton P.** cGMP-dependent activation of protein kinase G precludes disulfide activation: implications for blood pressure control. *Hypertension* 60: 1301–1308, 2012. doi:10.1161/HYPERTENSIONAHA.112.198754.

9. **Christman BW, McPherson CD, Newman JH, King GA, Bernard GR, Groves BM, Loyd JE.** An imbalance between the excretion of thromboxane and prostacyclin metabolites in pulmonary hypertension. *N Engl J Med* 327: 70–75, 1992. doi:10.1056/NEJM199207093270202.

10. **Ciuclan L, Bonneau O, Hussey M, Duggan N, Holmes AM, Good R, Stringer R, Jones P, Morrell NW, Jarai G, Walker C, Westwick J, Thomas M.** A novel murine model of severe pulmonary arterial hypertension. *Am J Respir Crit Care Med* 184: 1171–1182, 2011. doi:10.1164/rccm.201103-0412OC.

11. **Cruz JA, Bauer EM, Rodriguez AI, Gangopadhyay A, Zeineh NS, Wang Y, Shiva S, Champion HC, Bauer PM.** Chronic hypoxia induces right heart failure in caveolin-1$^{-/-}$ mice. *Am J Physiol Heart Circ Physiol* 302: H2518–H2527, 2012. doi:10.1152/ajpheart.01140.2011.

12. **Daut J, Maier-Rudolph W, von Beckerath N, Mehrke G, Günther K, Goedel-Meinen L.** Hypoxic dilation of coronary arteries is mediated by ATP-sensitive potassium channels. *Science* 247: 1341–1344, 1990. doi:10.1126/science.2107575.

13. **Dora KA, Gallagher NT, McNeish A, Garland CJ.** Modulation of endothelial cell KCa3.1 channels during endothelium-derived hyperpolarizing factor signaling in mesenteric resistance arteries. *Circ Res* 102: 1247–1255, 2008. doi:10.1161/CIRCRESAHA.108.172379.

14. **Enkhjargal B, Godo S, Sawada A, Suvd N, Saito H, Noda K, Satoh K, Shimokawa H.** Endothelial AMP-activated protein kinase regulates blood pressure and coronary flow responses through hyperpolarization mechanism in mice. *Arterioscler Thromb Vasc Biol* 34: 1505–1513, 2014. doi:10.1161/ATVBAHA.114.303735.

15. **Fagan KA, Fouty BW, Tyler RC, Morris KG Jr, Hepler LK, Sato K, LeCras TD, Abman SH, Weinberger HD, Huang PL, McMurtry IF, Rodman DM.** The pulmonary circulation of homozygous or heterozygous eNOS-null mice is hyperresponsive to mild hypoxia. *J Clin Invest* 103: 291–299, 1999. doi:10.1172/JCI3862.

16. **Feletou M.** Integrated systems physiology: from molecule to function to disease. In: *The Classical Pathway.* San Rafael, CA: Morgan & Claypool Life Sciences, part 2, 2011, p. 25.

17. **Félétou M, Girard V, Canet E.** Different involvement of nitric oxide in endothelium-dependent relaxation of porcine pulmonary artery and vein: influence of hypoxia. *J Cardiovasc Pharmacol* 25: 665–673, 1995. doi:10.1097/00005344-199504000-00022.

18. **Fike CD, Kaplowitz MR.** Chronic hypoxia alters nitric oxide-dependent pulmonary vascular responses in lungs of newborn pigs. *J Appl Physiol* 81: 2078–2087, 1996. doi:10.1152/jappl.1996.81.5.2078.

19. **Freed JK, Durand MJ, Hoffmann BR, Densmore JC, Greene AS, Gutterman DD.** Mitochondria-regulated formation of endothelium-derived extracellular vesicles shifts the mediator of flow-induced vasodilation. *Am J Physiol Heart Circ Physiol* 312: H1096–H1104, 2017. doi:10.1152/ajpheart.00680.2016.

20. **Galiè N, Brundage BH, Ghofrani HA, Oudiz RJ, Simonneau G, Safdar Z, Shapiro S, White RJ, Chan M, Beardsworth A, Frumkin L, Barst RJ; Pulmonary Arterial Hypertension and Response to Tadalafil (PHIRST) Study Group.** Tadalafil therapy for pulmonary arterial hypertension. *Circulation* 119: 2894–2903, 2009. doi:10.1161/CIRCULATIONAHA.108.839274.

21. **Garland CJ, Dora KA.** EDH: endothelium-dependent hyperpolarization and microvascular signaling. *Acta Physiol (Oxf)* 219: 152−161, 2017. doi:10.1111/apha.12649.

22. **Gebicka L, Didik J.** Catalytic scavenging of peroxynitrite by catalase. *J Inorg Biochem* 103: 1375–1379, 2009. doi:10.1016/j.jinorgbio.2009.07.011.

23. **Ghofrani HA, D'Armini AM, Grimminger F, Hoeper MM, Jansa P, Kim NH, Mayer E, Simonneau G, Wilkins MR, Fritsch A, Neuser D, Weimann G, Wang C; CHEST-1 Study Group.** Riociguat for the treatment of chronic thromboembolic pulmonary hypertension. *N Engl J Med* 369: 319–329, 2013. doi:10.1056/NEJMoa1209657.

24. **Ghofrani HA, Galiè N, Grimminger F, Grünig E, Humbert M, Jing ZC, Keogh AM, Langleben D, Kilama MO, Fritsch A, Neuser D, Rubin LJ; PATENT-1 Study Group.** Riociguat for the treatment of pulmonary arterial hypertension. *N Engl J Med* 369: 330–340, 2013. doi:10.1056/NEJMoa1209655.

25. **Ghosh S, Gachhui R, Crooks C, Wu C, Lisanti MP, Stuehr DJ.** Interaction between caveolin-1 and the reductase domain of endothelial nitric-oxide synthase. Consequences for catalysis. *J Biol Chem* 273: 22267–22271, 1998. doi:10.1074/jbc.273.35.22267.

26. **Giaid A, Saleh D.** Reduced expression of endothelial nitric oxide synthase in the lungs of patients with pulmonary hypertension. *N Engl J Med* 333: 214–221, 1995. doi:10.1056/NEJM199507273330403.

27. **Gluais P, Edwards G, Weston AH, Falck JR, Vanhoutte PM, Félétou M.** Role of SK$_{Ca}$ and IK$_{Ca}$ in endothelium-dependent hyperpolarizations of the guinea-pig isolated carotid artery. *Br J Pharmacol* 144: 477–485, 2005. doi:10.1038/sj.bjp.0706003.

28. **Godo S, Sawada A, Saito H, Ikeda S, Enkhjargal B, Suzuki K, Tanaka S, Shimokawa H.** Disruption of physiological balance between nitric oxide and endothelium-dependent hyperpolarization impairs cardiovascular homeostasis in mice. *Arterioscler Thromb Vasc Biol* 36: 97–107, 2016.

29. **Godo S, Shimokawa H.** Divergent roles of endothelial nitric oxide synthases system in maintaining cardiovascular homeostasis. *Free Radic Biol Med* 109: 4–10, 2017. doi:10.1016/j.freeradbiomed.2016.12.019.

30. **Hampl V, Tristani-Firouzi M, Hutsell TC, Archer SL.** Nebulized nitric oxide/nucleophile adduct reduces chronic pulmonary hypertension. *Cardiovasc Res* 31: 55–62, 1996. doi:10.1016/S0008-6363(95)00172-7.

31. **Huertas A, Perros F, Tu L, Cohen-Kaminsky S, Montani D, Dorfmüller P, Guignabert C, Humbert M.** Immune dysregulation and endothelial dysfunction in pulmonary arterial hypertension: a complex interplay. *Circulation* 129: 1332–1340, 2014. doi:10.1161/CIRCULATIONAHA.113.004555.

32. **Humbert M, Sitbon O, Chaouat A, Bertocchi M, Habib G, Gressin V, Yaïci A, Weitzenblum E, Cordier JF, Chabot F, Dromer C, Pison C, Reynaud-Gaubert M, Haloun A, Laurent M, Hachulla E, Cottin V, Degano B, Jaïs X, Montani D, Souza R, Simonneau G.** Survival in patients with idiopathic, familial, and anorexigen-associated pulmonary arterial hypertension in the modern management era. *Circulation* 122: 156–163, 2010. doi:10.1161/CIRCULATIONAHA.109.911818.

33. **Khavandi K, Baylie RA, Sugden SA, Ahmed M, Csato V, Eaton P, Hill-Eubanks DC, Bonev AD, Nelson MT, Greenstein AS.** Pressure-induced oxidative activation of PKG enables vasoregulation by Ca^{2+} sparks and BK channels. *Sci Signal* 9: ra100, 2016. doi:10.1126/scisignal.aaf6625.

34. **Khoo JP, Zhao L, Alp NJ, Bendall JK, Nicoli T, Rockett K, Wilkins MR, Channon KM.** Pivotal role for endothelial tetrahydrobiopterin in pulmonary hypertension. *Circulation* 111: 2126–2133, 2005. doi:10.1161/01.CIR.0000162470.26840.89.

35. **Kinashi Y, Takahashi S, Kashino G, Okayasu R, Masunaga S, Suzuki M, Ono K.** DNA double-strand break induction in Ku80-deficient CHO cells following boron neutron capture reaction. *Radiat Oncol* 6: 106, 2011. doi:10.1186/1748-717X-6-106.

36. **Kraehling JR, Hao Z, Lee MY, Vinyard D, Velazquez H, Liu X, Stan RV, Brudvig G, Sessa WC.** Uncoupling caveolae from intracellular signaling in vivo. *Circ Res* 115: 115–130, 2015.

37. **Lahm T, Crisostomo PR, Markel TA, Wang M, Weil BR, Novotny NM, Meldrum DR.** The effects of estrogen on pulmonary artery vasoreactivity and hypoxic pulmonary vasoconstriction: potential new clinical implications for an old hormone. *Crit Care Med* 36: 2174–2183, 2008. doi:10.1097/CCM.0b013e31817d1a92.

38. **Lai YC, Potoka KC, Champion HC, Mora AL, Gladwin MT.** Pulmonary arterial hypertension: the clinical syndrome. *Circ Res* 115: 115–130, 2014. doi:10.1161/CIRCRESAHA.115.301146.

39. **Lam CF, Van Heerden PV, Blott J, Roberts B, Ilett KF.** The selective pulmonary vasodilatory effect of inhaled DETA/NO, a novel nitric oxide donor, in ARDS-a pilot human trial. *J Crit Care* 19: 48–53, 2004. doi:10.1016/j.jcrc.2004.02.009.

40. **Leung SW, Vanhoutte PM.** Endothelium-dependent hyperpolarization: age, gender and blood pressure, do they matter? *Acta Physiol (Oxf)* 219: 108–123, 2017. doi:10.1111/apha.12628.

41. **Liu JQ, Zelko IN, Erbynn EM, Sham JS, Folz RJ.** Hypoxic pulmonary hypertension: role of superoxide and NADPH oxidase (gp91^{phox}). *Am J Physiol Lung Cell Mol Physiol* 290: L2–L10, 2006. doi:10.1152/ajplung.00135.2005.

42. **Mason NA, Springall DR, Burke M, Pollock J, Mikhail G, Yacoub MH, Polak JM.** High expression of endothelial nitric oxide synthase in plexiform lesions of pulmonary hypertension. *J Pathol* 185: 313–318, 1998. doi:10.1002/(SICI)1096-9896(199807)185:3<313::AID-PATH93>3.0.CO;2-8.

43. **Matoba T, Shimokawa H, Kubota H, Morikawa K, Fujiki T, Kunihiro I, Mukai Y, Hirakawa Y, Takeshita A.** Hydrogen peroxide is an endothelium-derived hyperpolarizing factor in human mesenteric arteries. *Biochem Biophys Res Commun* 290: 909–913, 2002. doi:10.1006/bbrc.2001.6278.

44. **Matoba T, Shimokawa H, Morikawa K, Kubota H, Kunihiro I, Urakami-Harasawa L, Mukai Y, Hirakawa Y, Akaike T, Takeshita A.** Electron spin resonance detection of hydrogen peroxide as an endothelium-derived hyperpolarizing factor in porcine coronary microvessels. *Arterioscler Thromb Vasc Biol* 23: 1224–1230, 2003. doi:10.1161/01.ATV.0000078601.79536.6C.

45. **Matoba T, Shimokawa H, Nakashima M, Hirakawa Y, Mukai Y, Hirano K, Kanaide H, Takeshita A.** Hydrogen peroxide is an endothelium-derived hyperpolarizing factor in mice. *J Clin Invest* 106: 1521–1530, 2000. doi:10.1172/JCI10506.

46. **Mattagajasingh I, Kim CS, Naqvi A, Yamamori T, Hoffman TA, Jung SB, DeRicco J, Kasuno K, Irani K.** SIRT1 promotes endothelium-dependent vascular relaxation by activating endothelial nitric oxide synthase. *Proc Natl Acad Sci USA* 104: 14855–14860, 2007. doi:10.1073/pnas.0704329104.

47. **Murata T, Lin MI, Huang Y, Yu J, Bauer PM, Giordano FJ, Sessa WC.** Reexpression of caveolin-1 in endothelium rescues the vascular, cardiac, and pulmonary defects in global caveolin-1 knockout mice. *J Exp Med* 204: 2373–2382, 2007. doi:10.1084/jem.20062340.

48. **Nakajima S, Ohashi J, Sawada A, Noda K, Fukumoto Y, Shimokawa H.** Essential role of bone marrow for microvascular endothelial and metabolic functions in mice. *Circ Res* 111: 87–96, 2012. doi:10.1161/CIRCRESAHA.112.270215.

49. **Nisbet RE, Graves AS, Kleinhenz DJ, Rupnow HL, Reed AL, Fan TH, Mitchell PO, Sutliff RL, Hart CM.** The role of NADPH oxidase in chronic intermittent hypoxia-induced pulmonary hypertension in mice. *Am J Respir Cell Mol Biol* 40: 601–609, 2009. doi:10.1165/2008-0145OC.

50. **Ohashi J, Sawada A, Nakajima S, Noda K, Takaki A, Shimokawa H.** Mechanisms for enhanced endothelium-derived hyperpolarizing factor-mediated responses in microvessels in mice. *Circ J* 76: 1768–1779, 2012. doi:10.1253/circj.CJ-12-0197.

51. **Oishi P, Grobe A, Benavidez E, Ovadia B, Harmon C, Ross GA, Hendricks-Munoz K, Xu J, Black SM, Fineman JR.** Inhaled nitric oxide induced NOS inhibition and rebound pulmonary hypertension: a role for superoxide and peroxynitrite in the intact lamb. *Am J Physiol Lung Cell Mol Physiol* 290: L359–L366, 2006. doi:10.1152/ajplung.00019.2005.

52. **Olschewski A, Papp R, Nagaraj C, Olschewski H.** Ion channels and transporters as therapeutic targets in the pulmonary circulation. *Pharmacol Ther* 144: 349–368, 2014. doi:10.1016/j.pharmthera.2014.08.001.

53. **Ozaki M, Kawashima S, Yamashita T, Ohashi Y, Rikitake Y, Inoue N, Hirata KI, Hayashi Y, Itoh H, Yokoyama M.** Reduced hypoxic pulmonary vascular remodeling by nitric oxide from the endothelium. *Hypertension* 37: 322–327, 2001. doi:10.1161/01.HYP.37.2.322.

54. **Petersson J, Zygmunt PM, Jönsson P, Högestätt ED.** Characterization of endothelium- dependent relaxation in guinea pig basilar artery - effect of hypoxia and role of cytochrome P450 mono-oxygenase. *J Vasc Res* 35: 285–294, 1998. doi:10.1159/000025595.

55. **Radi R.** Peroxynitrite, a stealthy biological oxidant. *J Biol Chem* 288: 26464–26472, 2013. doi:10.1074/jbc.R113.472936.

56. **Rubin LJ, Badesch DB, Barst RJ, Galie N, Black CM, Keogh A, Pulido T, Frost A, Roux S, Leconte I, Landzberg M, Simonneau G.** Bosentan therapy for pulmonary arterial hypertension. *N Engl J Med* 346: 896–903, 2002. doi:10.1056/NEJMoa012212.

57. **Satoh K, Satoh T, Kikuchi N, Omura J, Kurosawa R, Suzuki K, Sugimura K, Aoki T, Nochioka K, Tatebe S, Miyamichi-Yamamoto S, Miura M, Shimizu T, Ikeda S, Yaoita N, Fukumoto Y, Minami T, Miyata S, Nakamura K, Ito H, Kadomatsu K, Shimokawa H.** Basigin mediates pulmonary hypertension by promoting inflammation and vascular smooth muscle cell proliferation. *Circ Res* 115: 738–750, 2014. doi:10.1161/CIRCRESAHA.115.304563.

58. **Sheak JR, Weise-Cross L, deKay RJ, Walker BR, Jernigan NL, Resta TC.** Enhanced NO-dependent pulmonary vasodilation limits increased vasoconstrictor sensitivity in neonatal chronic hypoxia. *Am J Physiol Heart Circ Physiol* 313: H828–H838, 2017. doi:10.1152/ajpheart.00123.2017.

59. **Shimokawa H.** 2014 Williams Harvey Lecture: importance of coronary vasomotion abnormalities-from bench to bedside. *Eur Heart J* 35: 3180–3193, 2014. doi:10.1093/eurheartj/ehu427.

60. **Shimokawa H, Yasutake H, Fujii K, Owada MK, Nakaike R, Fukumoto Y, Takayanagi T, Nagao T, Egashira K, Fujishima M, Takeshita A.** The importance of the hyperpolarizing mechanism increases as the vessel size decreases in endothelium-dependent relaxation in rat mesenteric circulation. *J Cardiovasc Pharmacol* 28: 703–711, 1996. doi:10.1097/00005344-199611000-00014.

61. **Simonneau G, Barst RJ, Galie N, Naeije R, Rich S, Bourge RC, Keogh A, Oudiz R, Frost A, Blackburn SD, Crow JW, Rubin LJ; Treprostinil Study Group.** Continuous subcutaneous infusion of treprostinil, a prostacyclin analogue, in patients with pulmonary arterial hypertension: a double-blind, randomized, placebo-controlled trial. *Am J Respir Crit Care Med* 165: 800–804, 2002. doi:10.1164/ajrccm.165.6.2106079.

62. **Stephens RS, Rentsendorj O, Servinsky LE, Moldobaeva A, Damico R, Pearse DB.** cGMP increases antioxidant function and attenuates oxidant cell death in mouse lung microvascular endothelial cells by a protein kinase G-dependent mechanism. *Am J Physiol Lung Cell Mol Physiol* 299: L323–L333, 2010. doi:10.1152/ajplung.00442.2009.

63. **Sweeney L, Voelkel NF.** Estrogen exposure, obesity and thyroid disease in women with severe pulmonary hypertension. *Eur J Med Res* 14: 433–442, 2009. doi:10.1186/2047-783X-14-10-433.

64. **Takaki A, Morikawa K, Tsutsui M, Murayama Y, Tekes E, Yamagishi H, Ohashi J, Yada T, Yanagihara N, Shimokawa H.** Crucial role of nitric oxide synthases system in endothelium-dependent hyperpolarization in mice. *J Exp Med* 205: 2053–2063, 2008. doi:10.1084/jem.20080106.

65. **Thomas SR, Chen K, Keaney JF Jr.** Hydrogen peroxide activates endothelial nitric-oxide synthase through coordinated phosphorylation and dephosphorylation via a phosphoinositide 3-kinase-dependent signaling pathway. *J Biol Chem* 277: 6017–6024, 2002. doi:10.1074/jbc.M109107200.

66. **Townsend EA, Miller VM, Prakash YS.** Sex differences and sex steroids in lung health and disease. *Endocr Rev* 33: 1–47, 2012. doi:10.1210/er.2010-0031.

67. **Tuder RM, Cool CD, Geraci MW, Wang J, Abman SH, Wright L, Badesch D, Voelkel NF.** Prostacyclin synthase expression is decreased in lungs from patients with severe pulmonary hypertension. *Am J Respir Crit Care Med* 159: 1925–1932, 1999. doi:10.1164/ajrccm.159.6.9804054.

68. **Umar S, Rabinovitch M, Eghbali M.** Estrogen paradox in pulmonary hypertension: current controversies and future perspectives. *Am J Respir Crit Care Med* 186: 125–131, 2012. doi:10.1164/rccm.201201-0058PP.

69. **Urakami-Harasawa L, Shimokawa H, Nakashima M, Egashira K, Takeshita A.** Importance of endothelium-derived hyperpolarizing factor in human arteries. *J Clin Invest* 100: 2793–2799, 1997. doi:10.1172/JCI119826.

70. **Vanhoutte PM, Zhao Y, Xu A, Leung SW.** Thirty years of saying NO: sources, fate, actions, and misfortunes of the endothelium-derived vasodilator mediator. *Circ Res* 119: 375–396, 2016. doi:10.1161/CIRCRESAHA.116.306531.

71. **Wandall-Frostholm C, Skaarup LM, Sadda V, Nielsen G, Hedegaard ER, Mogensen S, Köhler R, Simonsen U.** Pulmonary hypertension in wild type mice and animals with genetic deficit in KCa2.3 and KCa3.1 channels. *PLoS One* 9: e97687, 2014. doi:10.1371/journal.pone.0097687.

72. **Xue C, Rengasamy A, Le Cras TD, Koberna PA, Dailey GC, Johns RA.** Distribution of NOS in normoxic vs. hypoxic rat lung: upregulation of NOS by chronic hypoxia. *Am J Physiol* 267: L667–L678, 1994. https://www.ncbi.nlm.nih.gov/entrez/query.fcgi?cmd=Retrieve&db=PubMed&list_uids=7528981&dopt=Abstract.

73. **Yada T, Shimokawa H, Hiramatsu O, Kajita T, Shigeto F, Goto M, Ogasawara Y, Kajiya F.** Hydrogen peroxide, an endogenous endothelium-derived hyperpolarizing factor, plays an important role in coronary autoregulation in vivo. *Circulation* 107: 1040–1045, 2003. doi:10.1161/01.CIR.0000050145.25589.65.

74. **Yada T, Shimokawa H, Hiramatsu O, Shinozaki Y, Mori H, Goto M, Ogasawara Y, Kajiya F.** Important role of endogenous hydrogen peroxide in pacing-induced metabolic coronary vasodilation in dogs in vivo. *J Am Coll Cardiol* 50: 1272–1278, 2007. doi:10.1016/j.jacc.2007.05.039.

75. **Yoo HY, Zeifman A, Ko EA, Smith KA, Chen J, Machado RF, Zhao YY, Minshall RD, Yuan JX.** Optimization of isolated perfused/ventilated mouse lung to study hypoxic pulmonary vasoconstriction. *Pulm Circ* 3: 396–405, 2013. doi:10.4103/2045-8932.114776.

76. **Zhao YY, Liu Y, Stan RV, Fan L, Gu Y, Dalton N, Chu PH, Peterson K, Ross J Jr, Chien KR.** Defects in caveolin-1 cause dilated cardiomyopathy and pulmonary hypertension in knockout mice. *Proc Natl Acad Sci USA* 99: 11375–11380, 2002. doi:10.1073/pnas.172360799.

77. **Zhao YY, Zhao YD, Mirza MK, Huang JH, Potula HH, Vogel SM, Brovkovych V, Yuan JX, Wharton J, Malik AB.** Persistent eNOS activation secondary to caveolin-1 deficiency induces pulmonary hypertension in mice and humans through PKG nitration. *J Clin Invest* 119: 2009–2018, 2009. doi:10.1172/JCI33338.